Functional interaction between SGK1 and the Glucocorticoid Receptor

*Tutorized by **Diego Álvarez de la Rosa***

*Research group/Grupo de investigación**: Fisiología***

Celular y Molecular de Receptores Nucleares y Canales iónicos.

Julián Weller Pérez

Máster de Biomedicina

Universidad de La Laguna

Dr. Diego Álvarez de la Rosa Rodríguez, coordinador del Grupo de Investigación Fisiología Celular y Molecular de Receptores Nucleares y Canales Iónicos.

CERTIFICO /CERTIFICAN

- Que el Trabajo Fin de Máster (TFM) titulado "Functional interaction between SGK1 and the Glucocorticoid Receptor" ha sido realizado bajo mi supervisión por D Julián Weller Pérez, matriculada en el Máster en Biomedicina, durante el curso académico 2022/23.

- Que una vez revisada la memoria final del TFM, doy mi consentimiento para ser presentado a la evaluación (lectura y defensa) por el Tribunal designado por la Comisión Académica de la Titulación.

- Que se ha indicado expresamente, a través del mecanismo de entrega de la memoria TFM por sede electrónica ULL, el deseo de hacer público o no los resultados del TFM.

Para que conste, se firma el presente certificado en La Laguna a

08/07/2023   Dr. Diego Álvarez de la Rosa Rodríguez.

Escuela de Doctorado y Estudios de Posgrado. Edificio Central. Campus Central. 38071 La Laguna.

C/ Delgado Barreto S/N. Tfno. (00 34) 922 31 9000
http://www.escuelas.ull.es/view/centros/escueladoctorado/Inicio· master@ull.es

INDEX

1. SUMMARY

El receptor de glucocorticoides (GR) se trata de un receptor nuclear que es capaz de regular la transcripción de los genes mediante la unión a glucocorticoides. Cuando este reconoce a su ligando, GR viaja al núcleo dónde dimeriza y se une al DNA en secuencias específicas conocidas como Elemento de respuesta de glucocorticoides (GRE), que permiten a GR regular la expresión génica. Entre las muchas funciones que cumple GR, tiene un importante papel en la adipogénesis, debido al control de la expresión génica de marcadores adipogénicos. Por otro lado, SGK1 es una quinasa muy vinculada con la vía PI3K y la señalización mediada por GR y MR; teniendo importantes roles en cáncer y en patologías como la resistencia de insulina o hipertrofia de tejido adiposo. En publicaciones recientes, se ha visto como SGK1 es capaz de inhibir la respuesta ejercida a través del receptor de estrógenos (ER), otro receptor nuclear; mediante un feedback negativo mediado por la remodelación de cromatina. Con esta premisa se pretende estudiar si SGK1 tiene un mecanismo de regulación similar con GR, empleando para ello cultivos primarios de fibroblastos embrionarios de ratón de cepas WT y cepas con SGK1 mutada como modelo de estudio.

Glucocorticoid receptor (GR) is a nuclear receptor able to regulate gene transcription by binding to glucocorticoids. Once GR binds to glucocorticoids, GR migrates to the nucleus and undergoes a dimerization process, binds to the DNA at Glucocorticoid Response Elements (GRE); which allows GR to regulate gene expression. Among many important functions GR fulfils, GR has a vital role in adipogenesis because it regulates the gene expression of several adipogenic markers. On the other hand, SGK1 is a kinase tightly linked to the PI3K pathway and GR and MR signalling; being an important protein in cancer and other pathologies like insulin resistance or hypertrophy of the adipose tissue. In recent studies, it has been demonstrated how SGK1 is capable of inhibiting estrogen receptor (ER) mediated response via negative feedback that involves chromatin remodelling. With this information as a premise, it will be the goal of this research to study if a similar mechanism is present between GR and SGK1, using mouse embryonic fibroblasts (MEFs) WT and MEFs with a mutated SGK1 as our model for research.

2. INTRODUCTION

2.1. THE GLUCOCORTICOID RECEPTOR (GR)

Nuclear receptors (NR) are a superfamily of proteins that act as ligand-binding transcriptional regulatory factors. The glucocorticoid receptor, or GR, encoded in humans by the *NR3C1* (Nuclear receptor subfamily 3 group C member 1) gene, is one of the most studied nuclear receptors along with other members of this steroid receptor subfamily like the mineralocorticoid receptor (MR, *NR3C2*), the progesterone receptor (PR: *NRC3*) or the androsterone receptor (AR, *NR3C4*) (Weikum et al. 2017).
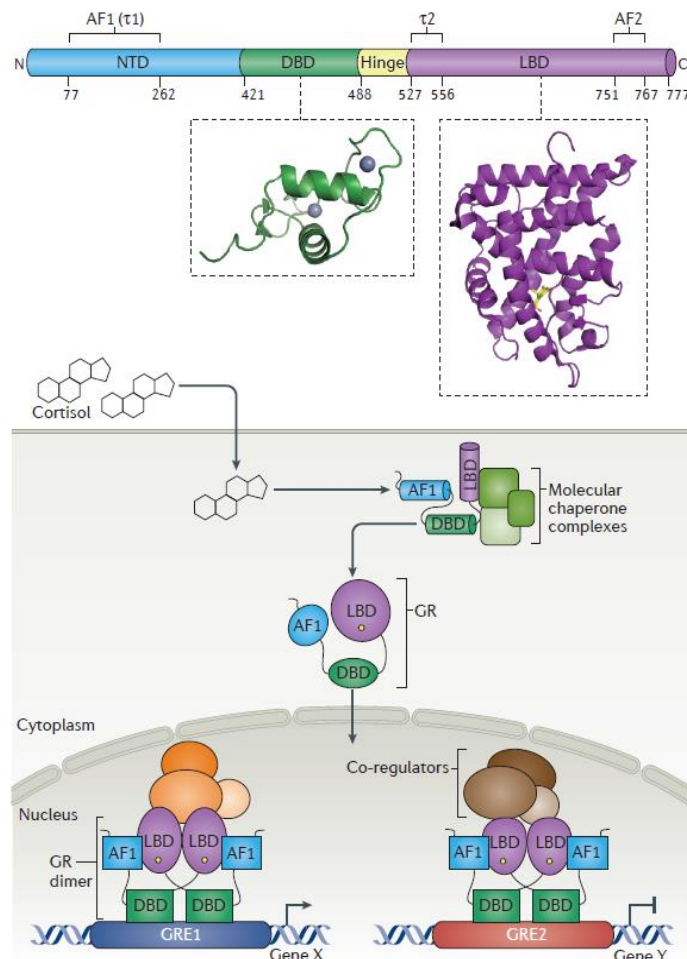

Figure 1. Glucocorticoid receptor domains and classical GR-signalling model (Weikum et al., 2017)

All these nuclear receptors share a common protein structure, characterized by the presence of three domains (Figure 1). These domains are the amino-terminal domain (NTD), a DNA binding domain (DBD) formed by two zinc-finger structures, and the carboxy-terminal ligand-binding domain (LBD). The NTD and LBD contain Activation Function Domains (AF1 and AF2) sequences that participate in the recruitment of transcriptional co-regulators. Although the LBD and DBD are highly conserved across the NR3C family, the AF1domain as well as the entire NTD region is highly diverse (Weikum et al. 2017).

Figure 1 shows a model of the mechanism of GR activation and function. Once the ligand is bound to the LBD, GR migrates to the nucleus and undergoes a dimerization process, and then binds to specific DNA sequences known as Glucocorticoid Response Elements

(GREs), where GR recruits cofactors that in turn regulate gene expression. Although one may think that these GREs have to be near the transcriptional start site (TSS) of the regulated gene, the truth is that GREs have been reported in a wide variety of distances from the TSS that can go up to several kb upstream or downstream (So et al. 2007). Furthermore, it has been reported that GR in the nucleus, once it binds to DNA, the dimer formed undergoes a series of conformational changes in the LBD that promotes the formation of a tetramer of GR dimers, as we can see in Figure 2 (Presman et al. 2016). This adds another layer of complexity to GR regulation and function, because, as the figure illustrates, this tetrameric conformation may bring distant GREs sites to close proximity, which in turn may have an impact on the regulation of gene expression.
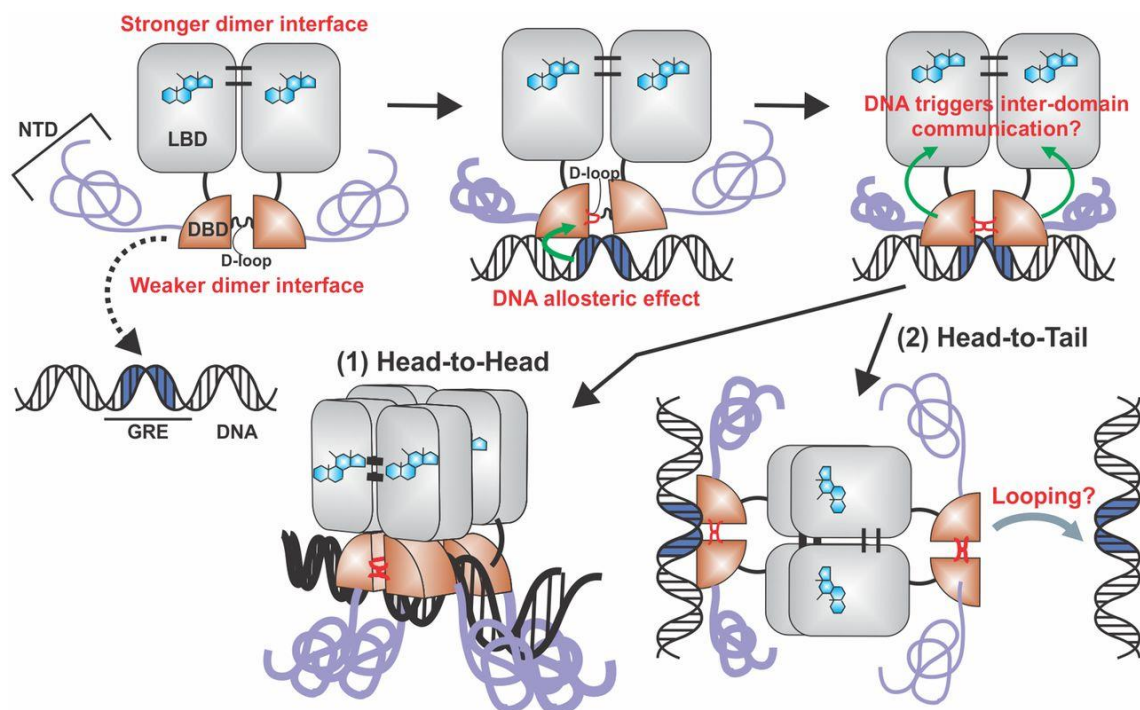

Figure 2. Proposed model for GR tetramerization (Presman et al. 2016)

Additionally, GR signalling and regulation is even more complex when it is taken into account the isoforms that can generate from the GR gene. In humans, *NR3C1* is located on chromosome 5 (5q31-32), having a total of 9 exons. Two isoforms arise from alternative splicing, hGRα (human GRα) and hGRβ. These two isoforms differ in the C-terminal domains, with the β isoform presenting a shorter domain than the α isoform, as seen in Figure 3 (Kadmiel y Cidlowski 2013). These isoforms are also present in mice (Hinds et al. 2010). GRα follows the activation mechanism described above (Figure 1), binding glucocorticoids in the cytoplasm, migrating to the nucleus and there regulating

gene expression. On the other hand, GRβ resides in the nucleus constitutively and functions as a negative regulator of the α isoform (Kadmiel y Cidlowski 2013)
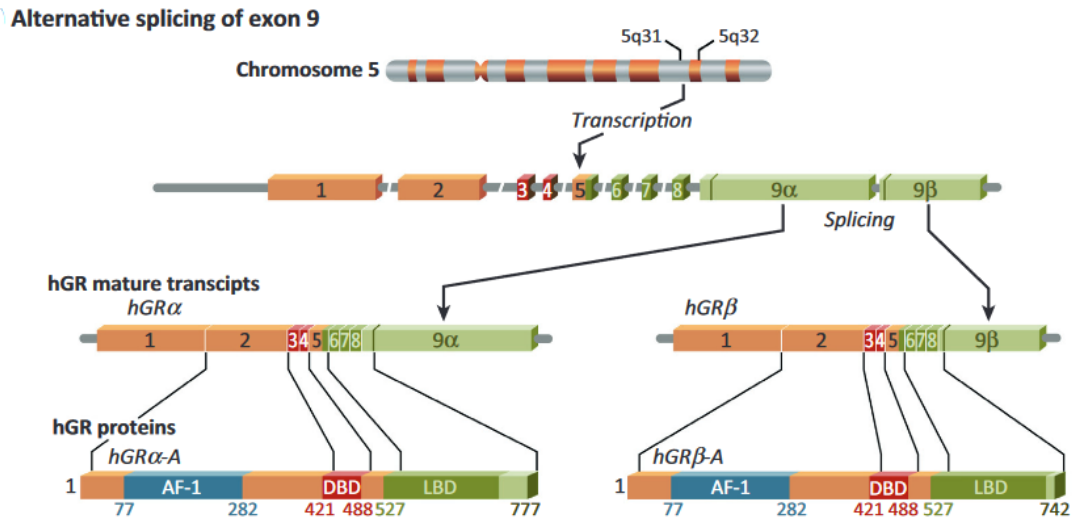

Figure 3. NR3C1 genomic location and different splicing leading to splicing isoforms hGRα and hGRβ (Kadmiel y Cidlowski 2013).

2.1.1. GR ROLE IN ADIPOGENESIS

Adipogenesis is understood as the process in which fibroblast-like adipocytes develop into insulin-responsive adipocytes as presented in Figure 4 (Ali et al. 2013).
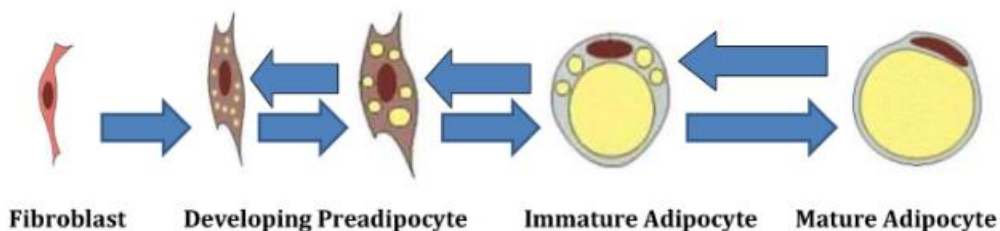
Figure 4. Adipocyte differentiation process. Backward arrows illustrate adipocyte shrinking dure to weight loss processes. (Ali et al. 2013)

This differentiation process is tightly regulated in terms of gene expression and molecular markers of adipogenesis have been identified. Some of these molecular markers are peroxisome proliferation-activated receptor γ (*PPARγ*) or the enhancer-binding proteins

Figure 5. CEBPs and PPARγ dynamics in adipogenesis. (Lefterova & Lazar, 2009)

α, β and δ (*CEBPα/β/δ*), being CEBPβ and δ the ones that promote PPARγ expression in early adipogenesis expression (Figure 5, Lefterova & Lazar, 2009). GR signalling has been demonstrated to have an important role in *in vitro* adipogenesis as it has been shown that dexamethasone (DE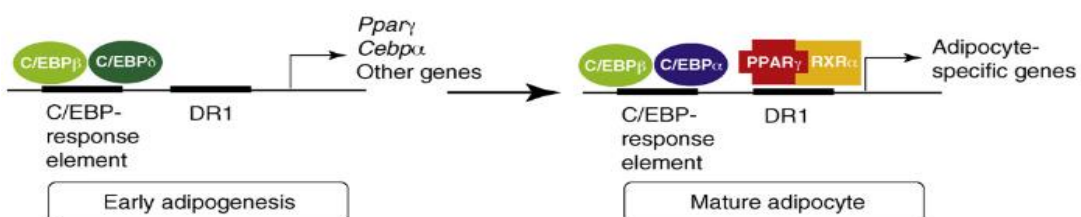X, an agonist of GR; LaLone et al., 2012) treatment on MEFs mouse embryonic fibroblasts (MEFs) induces CEBPβ expression and therefore PPARγ. This is reinforced by the fact that MEFs treated with GR antagonists and MEFs lacking GR expression have impaired *in* vitro adipogenesis (Bauerle et al. 2018).

2.2. SERUM AND GLUCOCORTICOID-REGULATED KINASE 1 (SGK1)

The serum and glucocorticoid-regulated kinase 1 (SGK1) is a serine/threonine kinase present in humans and mice (encoded by *SGK1* and *Sgk1* respectively) (Kobayashi et al. 1999) that belongs, along with SGK2 and SGK3 to the SGK kinase family. SGKs are in turn part of the AGC kinase superfamily, which includes AKT or PDK1 (Ghani 2022), proteins that have a vital role in important signalling pathways like the PI3K-AKT-mTor pathway (Cerma et al. 2023).

SGK1 owns its name because its expression is up-regulated, at least in part, by the activation of GR. This is explained by the presence of a GRE approximately 1 kb upstream of the TSS (Webster et al. 1993). Apart from this transcriptional regulation by GR, SGK1 also presents regulation at posttranscriptional levels. SGK1 needs to be activated after being synthesised. To achieve its active state, SGK1 needs phosphorylation by the
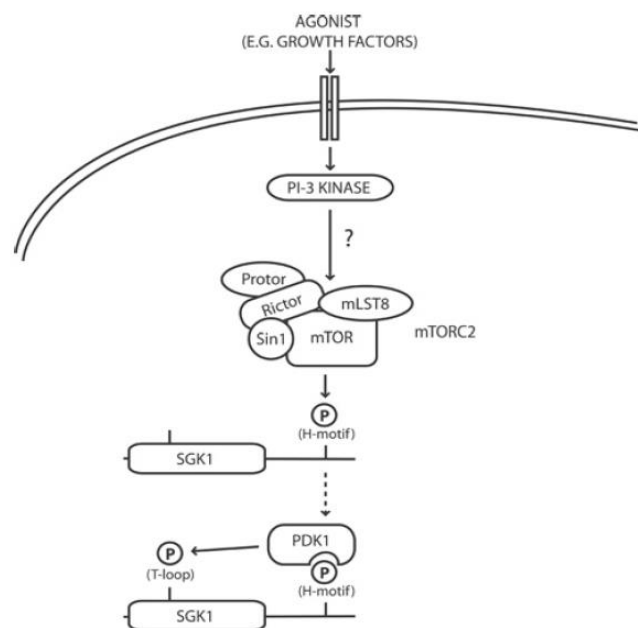
Figure 6. SGK1 activation process is mediated by PI3K pathway. (García-Martínez & Alessi, 2008)

mammalian Target of Rapamycin Complex 2 (mTORC2) at the S422 residue, which is located in SGK1 hydrophobic motif. This phosphorylation allows PDK1 to interact with SGK1 hydrophobic motif and phosphorylates SGK1 once again at T256, which is located in the T-loop at the kinase domain, making it active (Figure 6; García-Martínez & Alessi, 2008).

In many cancer types, the PI3K/AKT/mTOR pathway is altered or up-regulated, resulting in a wide variety of pathophysiological characteristics found in cancer cells (Ghani 2022; Zhu et al. 2020). This pathway upregulation leads to an increase in SGK1 activity because of its activation mechanism. The resulting SGK1 up-regulation leads to cancer cell proliferation mediated by PI3K activation due to the inhibition of mTOR. SGK1 increased activity leads to phosphorylation of the transcription factor Foxo3a, a protein that can induce cell cycle arrest and apoptosis (Zhu et al. 2020).

In recent years, SGK1 has been attributed to be responsible for the development of resistance in cancer cells upon PI3K inhibition and recent studies show how inhibition of AKT alongside SGK1 has a higher suppression rate on tumours (Castel et al. 2016; Orlacchio et al. 2017). This is probably because of the high similarity in structure in the catalytic site of both enzymes (Toska et al. 2019) and that both kinases share the same phosphorylation motif (RXRXXS/T)(Alessi, Pearce, y García-Martínez 2009).

In addition to its role in cancer, SGK1 has been implicated in a wide variety of process, including its role as a downstream target of GR and MR signaling. In adipocytes, SGK1 activity promotes hypertrophy and insulin resistance, contributing to the development of metabolic syndrome (Sierra-Ramos et al. 2020).

2.2.1 SGK1 and NR feedback

It was observed in Toska et al., 2019 that the increased expression of SGK1 upon PI3K inhibition is mediated by the estrogen receptor (ER, *NC3A1)*. Because of the inhibition of AKT due to PI3K inhibition, the kinase stops phosphorylating KMT2D, which is a chromatin remodeler that upon AKT-phosphorylation diminishes its activity (Toska et al. 2017). When PI3K is inhibited, KMT2D is not phosphorylated, making loci containing ERE (Estrogen Response Elements) accessible to ER. This promotes the SGK1 expression, as mentioned before. But once SGK1 is expressed and activated by PDK1 and mTORC2, because of the similarity of catalytic site between SGK1 and AKT, SGK1 phosphorylates KMT2D, inhibiting ER-dependent transcription (Figure 7, Toska et al., 2019).

Taking all this information into account, we wondered if GR, also being a nuclear receptor as ER, and also having a regulatory role in SGK1 expression (as SGK1 does have a GRE), could have a regulatory feedback interaction with the kinase.
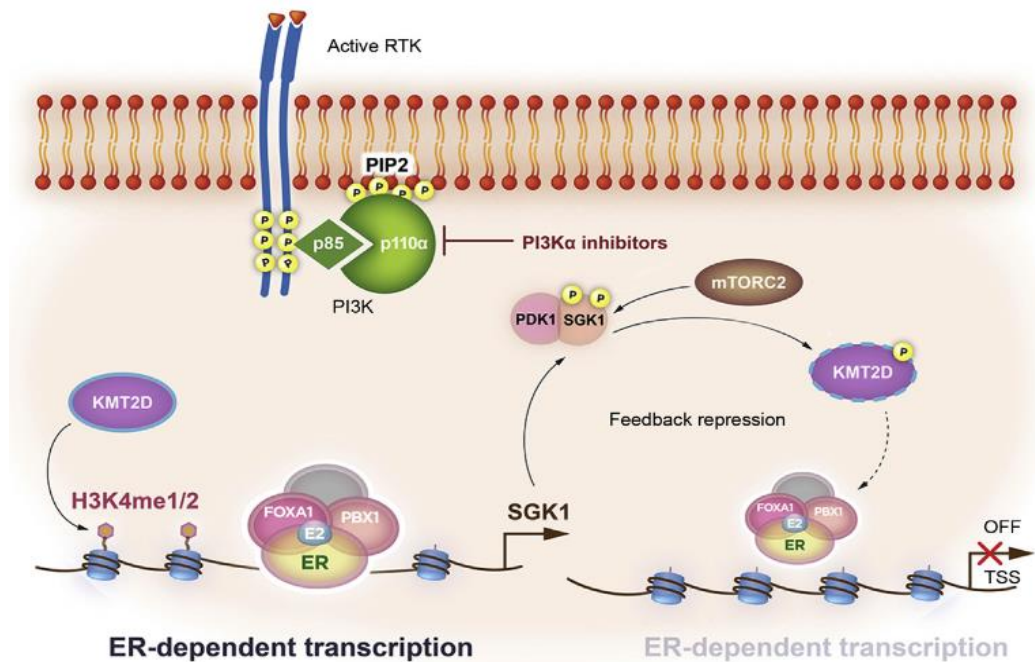
Figure 7. PI3K inhibition induces ER-dependent transcription that is down-regulated by SGK1 via negative feedback. (Toska et al., 2019)

3. HYPOTHESIS AND OBJECTIVES

In this study, we hypothesized that SGK1 regulates GR activity, whether by an indirect mechanism or via a direct interaction, thereby altering glucocorticoid-regulated gene expression.

With this in mind, we propose the following two specific objectives:

1. To determine whether SGK1 affects GR-regulated gene expression and the possible molecular mechanisms involved in this effect.
2. To study phenotype changes in adipogenesis that can be caused by the functional GR-SGK1 interaction.

4. MATERIALS AND METHODS

4.1. MEF harvesting and culture

MEFs (mouse embryonic fibroblast) were harvested from pregnant C57 WT or transgenic SGK1 (Tg.SGK1) mice. Tg.SGK1 mice harbour a stable insertion of a bacterial artificial chromosome (BAC) containing 180 kbp of the mouse genome covering the entire SGK1 gene and associated regulatory elements. This BAC was modified by homologous recombination in E. coli to introduce a phospho-mimetic mutation (S422D) that mimics the phosphorylation that mTORC2 carries on SGK1, making SGK1 constitutively active

(Sierra-Ramos et al. 2020). MEFs were obtained within a 3-day window that covers embryonic days 13.5 to 15.5 following a previously described protocol (Qiu et al. 2016). The moment a vaginal plug is observed is considered as the embryonic day 0.5 (E 0.5). After euthanizing the pregnant mice, the uterus was removed and then placed on a 100 mm plate containing 10 ml of ice-cold PBS (Phosphate Buffered Saline) to extract each embryo with its yolk sac. Embryos were then transferred to a new 30 mm plate with cold PBS, where they were visually inspected looking for any structural alterations. If the embryos passed this visual inspection, the head and internal organs were removed as efficiently as possible. Following this step, the cleaned embryos were transferred to a new 30 mm dish containing 0.5 ml of rinsing medium, consisting on a mixture of Dulbecco's Modified Eagle Medium (DMEM; high glucose formulation) and 1% penicillin/streptomycin (Biowest, France), where the embryos were minced with a sterile razor. The fragments were then transferred to a 50 ml Falcon tube containing 5 ml of trypsin-EDTA (Biowest, France), pipetting up and down with a 5 ml serological pipette to help disaggregate the tissue. After 1-2 hours at 37ºC in a water bath, 5ml of rinsing medium were added to the tube and the cells recovered by centrifugation at 1200 x g for 5 minutes at room temperature. With a 5ml pipette, the whole pellet was resuspended in 1-2ml of the supernatant and then transferred to a T75 flask or 100 mm culture dish containing 10 ml of complete growth medium: DMEM High Glucose, 10% fetal bovine serum (FBS; Biowest, France) and 1% penicillin/streptomycin. The medium was changed the following day and cells were passed when reached 80-100% confluence using trypsin-EDTA and standard procedures.

4.2. Adipocyte differentiation and lipid droplet staining

Following Al-Sayegh et al., 2020, WT and Tg.SGK1 MEFs were grown in an adipogenic medium for 6 days with medium changes every 2 days. The adipogenic medium consisted on complete DMEM supplemented with 10 μg/ml insulin, 2 μM dexamethasone (DEX), 0.5 mM 3-isobutyl-1-methylxanthine (IBMX), and 25 μg/ml ascorbic acid. Lipid droplet staining was performed on differentiated MEF cells on a 6-well plate. Each well was washed once with 1 ml PBS and then fixed with 2.4 ml of 4% paraformaldehyde (PFA) for 5 minutes, then replaced with another 2,4 ml 4% PFA and further incubation for 1 hour at room temperature. After the incubation time, the PFA was aspired and each well was washed once with 2.4ml of 60% isopropanol. Wells were allowed to completely dry after removing the alcohol to ensure that the staining solution works properly. Each well

was incubated for 10 min with 1 ml of Oil Red-O (Sigma-Aldrich, Missouri) solution (six parts Oil Red-O and 4 parts H_2O) and then washed four times with water before observation under an inverted microscope.

4.3. Cell treatment and RNA extraction

For each of the four cell types acquired after MEFs extraction and adipocyte differentiation (MEF WT, MEF Tg.SGK1, differentiated WT adipocytes and differentiated Tg.SGK1 adipocytes), a total of six 100 mm culture dishes for each cell line were seeded and grown until near confluence was reached. At this point, the medium is aspirated and cells are washed once with PBS and replaced with DMEM supplemented with charcoal stripped FBS (CS, Biowest, France). Cells were left overnight in this medium and the following day the CS-DMEM medium was changed once again. Three of the six culture dishes had their medium changed to CS-DMEM with the addition of 100% ethanol in a proportion of 1:1000. The three remaining culture dishes had their medium changed to a CS-DMEM medium supplemented with 100 nM DEX, a concentration that fully activates GR (Hellal-Levy et al. 1999). After this final medium change, cells were incubated for 2 h and washed three times with PBS. For RNA extraction, the commercial kit NucleoSpin RNA (Macherey-Nagel) was used following the manufacturer's instructions. RNA sample concentrations were measured by absorption spectroscopy with a NanoDrop 2000 apparatus (Thermofisher, US) and then samples were labelled and stored at -80ºC for future use.

4.4. cDNA synthesis and qPCR

For cDNA synthesis, 1 µg of each RNA sample was used in the reaction mix, to have the same amount of cDNA from every sample. The kit used for this was the iScript cDNA kit (Biorad, US) and a cDNA program with the T100 Thermal Cycler was run (Biorad, US). Quantitative reverse transcription PCR (qPCR) reactions targeting several genes of interest were run with the CFX96 Touch Real-Time PCR Detection System (Biorad, US) with the following conditions:

1. 95 ºC for 3 minutes.
2. 95 ºC for 5 seconds
3. 65º for 15 seconds
4. 62 ºC for 15 seconds and read the plate. Go back to step 2 40 times.

Each sample of qPCR reaction mix consisted of 1 µl of cDNA sample, 10 µl of iQ SYBR Green Supermix (Biorad, US), 8,93 µl of free nuclease H_2O and 0,07 µl of 10 µM forward and reverse primers, with a total volume of 20 µl. All primers used in qPCR reactions appear in Table 1. Each sample was replicated three times per qPCR run. Quantitative analysis was performed using the ΔΔCt method and *Actb* (β-actin mouse gene) as the housekeeping gene.

TARGET GENE	PRIMER	SEQUENCE
Sgk1	Forward	GAAACAGAGAAGGATGGGCCTGAAC
	Reverse	GATCTCAGCTCCAGCACCACCAC
Actb	Forward	AGTGTGACGTTGACATCCGTA
	Reverse	AGTGTGACGTTGACATCCGTA
Per1	Forward	GAGCCCCAGGAGTGAAGAAA
	Reverse	CACTGACACCCCTTTTGGTC
Serpine1	Forward	CCGAGAGCTTTGTGAAGGAG
	Reverse	GAGGGTGAGAGATGGAGACG
Tsc22d3	Forward	CAGCGCAAGGCTAGCTAGCTA
	Reverse	CCATCTCCTTCTTTTCTTCTCTGCTTG
Cd36	Forward	AGATGACGTGGCAAAGAACAG
	Reverse	CCTTGGCTAGATAACGAACTC
Pparg	Forward	GTGCCTTGCTGTGGGGATGTC
	Reverse	CAAATGCTTTGCCAGGGCTCG

Table 1. Primers used on qPCR reactions of RNA samples

To study primer efficiency, each primer was tested with a qPCR run of standards from each cDNA synthesis reaction. The standards were made by pooling cDNAs from each sample and then diluted serially 1:4 and 1:16. The Ct obtained from the three standards was then represented against the $\log_{10}$ of the dilutions (1, 1/4 and 1/16). The slope that we get from the graphic is then put in a primer efficiency calculator to get the efficiency. If the efficiency is above 90% no corrections in the ΔΔCt analysis were applied.
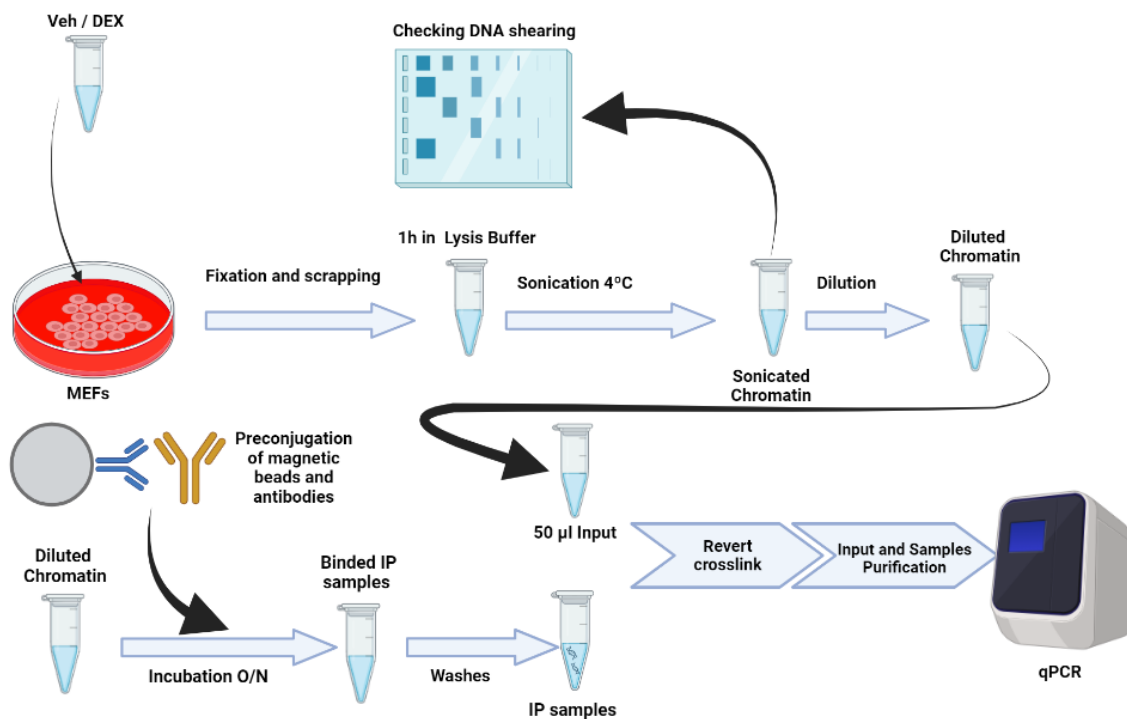
4.5. Chromatin Immunoprecipitation (ChIP)

Figure 8. ChIP protocol overview

ChIP was performed following the protocol stablished by the group of Dr. Gordon L. Hager (Laboratory of Receptor Biology and Gene Expression, National Cancer Institute, NIH, USA), as summarized in Figure 8. Cells were grown in 150 mm culture plates (ideally 2-3 plates per condition) and let reach 80-90% confluence. Just like with the RNA extraction plates, at this point cells were washed once with PBS and the medium was changed to CS-DMEM and incubated overnight. The following day medium was changed once again to CS-DMEM with 0.1% pure ethanol or 100 µM DEX for each condition and incubated for 1 h. Then 16% PFA (Thermofisher, US) was added to the medium to 1% final concentration while tilting the plates to mix medium and PFA fast. Cells were incubated at RT for 5 minutes and then glycine at a 20X (2.5 M) concentration was added to 1X. Cells were incubated for another 5 minutes at room temperature before being washed thrice with cold PBS. PFA crosslinks DNA-protein complexes that regulate DNA transcription and the glycine minimizes the crosslinks that may occur due to free PFA leftover in the medium, acting as a crosslink quencher (Figure 9, Hoffman et al., 2015).
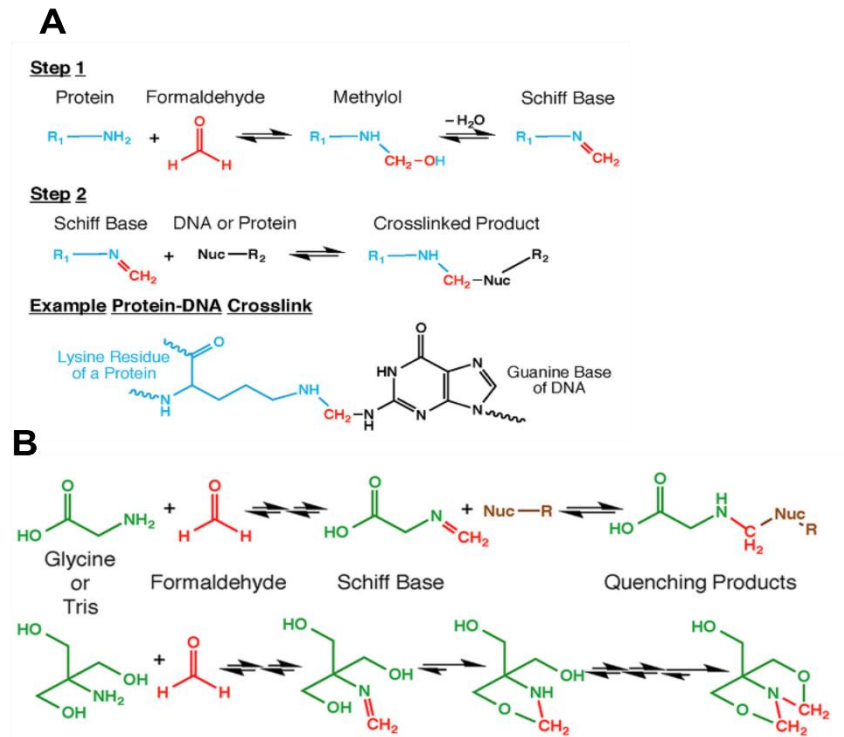
A

Step 1

Protein Formaldehyde Methylol Schiff Base

Step 2

Schiff Base DNA or Protein Crosslinked Product

Example Protein-DNA Crosslink

Lysine Residue of a Protein Guanine Base of DNA

B

Glycine or Tris Formaldehyde Schiff Base Quenching Products

Figure 9. A) Molecular mechanism of DNA-protein crosslinking. B) Molecular mechanism of glycine quenching. (Hoffman et al., 2015)

After these washes, 2.5 ml PBS containing protease inhibitors (cOmplete Protease Inhibitor Cocktail, Roche, Switzerland) was poured onto the plates. Cells were scraped off the dishes, collected in 15 ml conical tubes (cells with the same condition are collected in the same tube), and left in ice before pelleting the cells at 500 x *g* for 10 minutes at 4 ºC. The supernatant is aspirated and the pellet is resuspended in ChIP lysis buffer (0.5% SDS, 10mM EDTA, 50mM Tris-HCl pH8) with protease inhibitors (cOmplete, Roche) for 1 hour. Then, samples were split in 500-700 aliquots into 15 ml polystyrene conical tubes (Corning, USA) for the sonication process. A cleaned metal probe is inserted into the tubes and then put in the sonicator (Bioruptor, Diagenode). Sonication conditions were as follows: temperature set to 4ºC, power set to low and then 15 seconds ON and 7 seconds OFF for 9 cycles. Samples were transferred to Eppendorf tubes and then spun down for 5 minutes at 14000 rpm at 4ºC. The supernatant was collected and its volume was noted. Fifteen µl of the cleared samples were used to check chromatin shearing. To that end, samples were mixed with 180 µl of a master reversal mix of was prepared (50 mM Tris pH7, 222 mM NaCl, 10 mM EDTA) and 2,5 µl of 20 µg/µl Rnase A (REAL, Spain) were added. Fifteen µl of lysis buffer with protease inhibitors was used as a blank for this process. Samples were incubated for 30 minutes in a thermomixer at 37ºC, and then 2,5 µl of 20 mg/ml proteinase K (Qiagen, Germany) was added to each sample.

Samples were incubated another 30 min in the thermomixer at 50 ºC. After the incubation, we checked chromatin concentration using the previously mentioned NanoDrop 2000 and inferred the original sample concentration. Then samples were put in the thermomixer for 1 hour at 50 ºC and at least 7 hours at 65ºC to reverse crosslinks. To separate genomic DNA and proteins, a phenol-chloroform protocol was implemented with the use of Phaselock tubes (Quanta Bioscience, US) and ethanol precipitation. For each sample, a mixture of 5 µl purified chromatin samples, 5 µl H_2O and 2 µl of 6X loading dye was run alongside 5 µl of DNA ladder (peqGOLD, VWR) on a 1% agarose gel electrophoresis to check average chromatin size, which should be around 500 bp.

Once chromatin shearing was checked, original samples were diluted at least 5-fold in ChIP dilution buffer (CDB: 0.01% SDS, 1.1% Triton X-100, 1.2 mM EDTA, 16.7 mM Tris-HCl, and 167 mM NaCl) with protease inhibitors (cOmplete) to a final concentration of 800 µg/ml of chromatin. From each of these diluted samples, 50 µl were saved in Eppendorf tubes. For the next step, we pre-conjugated a magnetic bead suspension carrying protein G (Sigma-Aldrich, US) with an antibody against GR (G5, Santa Cruz Biotechnology), preparing 30 µl of beads per sample. To that end, beads were washed twice with 500 µl CDB and then incubated for 6 hours with 2 µl of G5 antibody at 4ºC with rotations. With a magnetic rack, the supernatant was removed, the conjugated beads washed twice with 500 µl CBD and then resuspend in 30 µl of CDB. The ChIP sample was added to the bead solution, leaving the mix overnight at 4 ºC with rotation. After the overnight incubation, ChIP samples were washed with the following sequence of buffers, using 800 µl of volume and 5 minutes at 4 ºC with rotation for each step:

1. Low salt immune complex buffer: 0.1% SDS, 1% Triton x-100, 2mM EDTA, 20mM Tris HCl pH8, 150mM NaCl
2. High salt immune complex buffer: 0.1% SDS, 1% Triton x-100, 2mM EDTA, 20mM Tris HCl pH8, 500mM NaCl
3. LiCl immune complex buffer: 0.25M LiCl, 1% NP-40, 1% deoxycholate, 1mM EDTA, 10mM Tris-HCl pH8
4. 1X TE: 10mMTris-HCl, 1mM EDTA pH8
5. 1X TE

After these washes, the supernatant was removed and 200 µl of reversal mix (200mM NaCl, 50 mM Tris 7.0, 10 mM EDTA, 0.0075% SDS and 50 µg Proteinase K) was added to the washed IP samples. The 50 µl that were saved before from each IP sample (Input),

150 µl of reversal mix was added as well. All samples were incubated for 2 hours at 50ºC and 65ºC at least 7 hours to reverse crosslinking. After crosslink reversal, samples were spun down and the liquid at the bottom of the tubes was collected into a screw-cap tube. In these tubes, 200 µl phenol-chloroform was added, vortexed vigorously for 60 seconds and then transferred to Phaselock tubes. Samples were centrifuged at max speed for 10 minutes at 4 ºC and the supernatant was saved. To each sample, 19 µl of sodium acetate/glycogen mix (18ul of sodium acetate 3M and 1 µl of a 20 µg/µl glycogen solution) was added, then vortexed and spun down. The next step involved adding to the samples 2.25 times the sample volume of cold pure ethanol and incubating the samples for 1 hour at -20 ºC. After this, samples were centrifuged at max speed for 30 minutes at 4 ºC, the supernatant was removed and then the resulting pellet was washed with 600 µl of 70% ethanol. The ethanol was carefully removed and the samples were left to dry completely before resuspending the pellet in 40 µl H_2O. Samples were stored at -20 ºC until further use. These samples were used in qPCR reactions in the same way as previously explained. Primers used for qPCR analysis of ChIP reactions are listed in Table 2 and flank or start in Glucocorticoid Response Elements (GRE) associated with the listed genes. ChIP-qPCR samples were analysed subtracting every average sample Ct with the average Ct obtained from the WT vehicle sample, resulting in a normalized ΔCt value. Input samples were used as a correction when Cts obtained in the input were not homogeneous.

TARGET GENE	PRIMER	SEQUENCE
Sgk1	Forward	CCCTCTAACTCGCCACCTCCTCACG
	Reverse	GGGGTCAGGAATGTGTAGGGGAGGG
Per1	Forward	GGGACCCCCTTCCTCCTAAC
	Reverse	AGCGCACTAGGGAACATCGT
Ampd3	Forward	CAGCGCAAGGCTAGCTAGCTA
	Reverse	CCATCTCCTTCTTTTCTTCTCTGCTTG
	Forward*	TTGATTCCAGCTTTTCATGCCAGAC
	Reverse*	AGTGGATTTCGGGATGACCTATGAT
Pdk4	Forward	TTTGTTACAAGGAACAACTTCATTTGGTGG
	Reverse	GGCATTGCTCTAACTCTCTCATACTTTC
Fkbp5	Forward	TTTGTTACAAGGAACAACTTCATTTGGTGG
	Reverse	GGCATTGCTCTAACTCTCTCATACTTTC

Table 2. Primers used on qPCR reaction of ChIP samples

5. RESULTS AND DISCUSSION

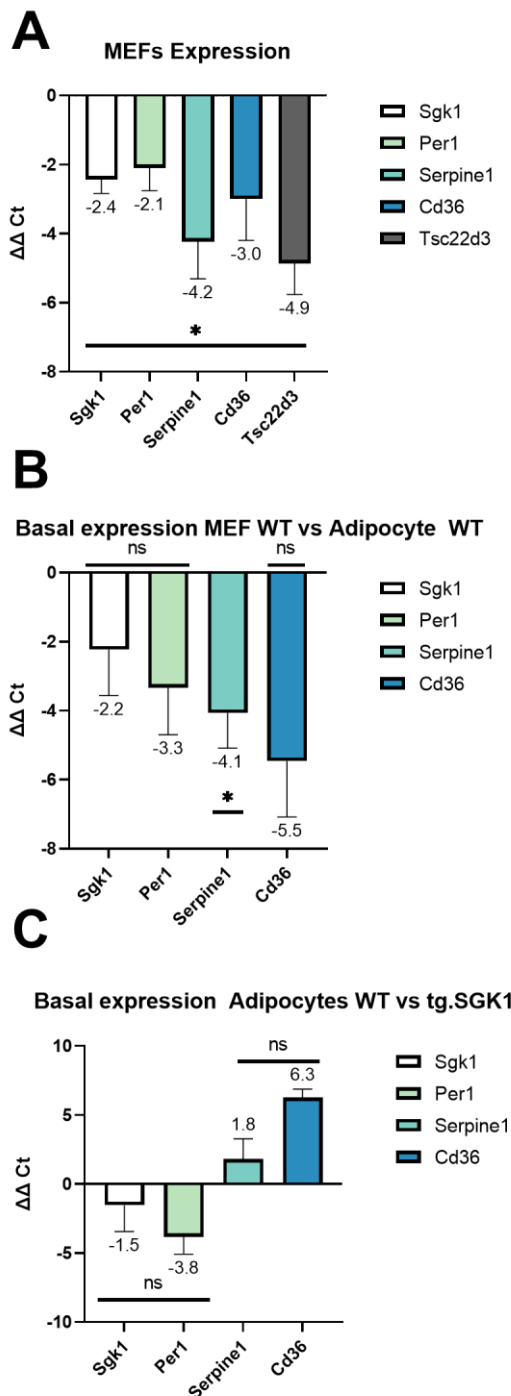## 5.1. Effect of increased SGK1 activity on GR gene targets

*Figure 10. Representation of the average change in the basal expression of the indicated genes between WT and Tg.SGK1 MEFs (A), WT MEFs and WT adipocytes (B) and WT and Tg.SGK1adipocytes (C). Differences are expressed as ΔΔCt, which is a logarithmic scale. * p-value < 0.05 using Students T-test comparing samples to MEFs WT vehicle samples (A and B) and Adipocytes WT vehicle (C)*

We first studied whether there are differences in the basal expression of selected GR-target genes when we compare the different cell types we have cultured. The differences observed are expressed as ΔΔCt (Threshold cycle) values, which indicate how many times the expression of the studied genes is higher or lower between the samples we are comparing. Due to the nature of what the Ct represents, when calculating the ΔΔCt it is worth reminding that negative values represent an increase of expression compared to the control sample, whereas a positive value indicates decreased expression. The actual fold-change value can be found using $2^{-(\Delta\Delta Ct)}$, but for simplicity and condensing of the data obtained, results are shown in ΔΔCt.

Figure 10. A) shows that all genes studied have significantly increased basal expression in Tg.SGK1 MEFs compared to WT MEFs. Genes used for this qPCR were selected due to its

known regulation by GR (Abumrad et al. 1993; Bereshchenko et al. 2019; Glatz y Luiken 2018; Knoedler et al. 2021; Pavlatou et al. 2013). This suggests that constitutively active SGK1 in transgenic MEFs may affect GR signalling, or another mechanism common to the regulation of all these genes, which translates into the increased basal expression registered in the analysis. It is worth saying that *Tsc22d3* expression is probably underestimated. This gene is not detected in WT samples, but to be able to quantitate a relative increase we set MEFs WT vehicle *Tsc22d3* Ct to a 40 Ct, making the analysis possible for this gene.

Differentiation of WT MEFs to adipocytes occur with increased expression of *Serpine1* (Figure 10B). Although the only statistically significant data is the one from *Serpine1*, it is worth mentioning that the other three genes tested show a tendency towards increased expression. In particular, we expected to detect increased levels of *Cd36*, since this gene encodes a transmembrane glycoprotein that participates in fatty acid uptake (Glatz y Luiken 2018), therefore having an important role in the adipose tissues and cells. Expression of Cd36 was variable, perhaps indicating an uneven differentiation of MEFs to adipocytes in each well. In both WT MEFs and adipocyte samples, *Tsc22d1* was undetectable.

We next compared the expression of selected genes between WT and transgenic adipocytes (Figure 10C). No statistically significant differences were observed between both groups, as opposed to the undifferentiated MEFs.
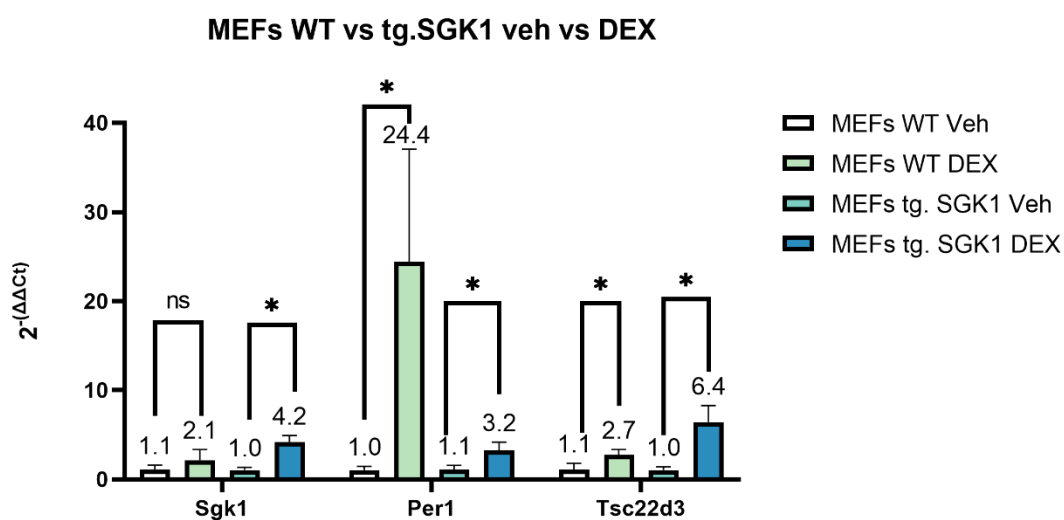

*Figure 11. Representation of modifications in gene expression after treatment with DEX data is represented as means. * p-value < 0.05 using Students T-test*

Until now our analysis has focused on basal gene expression in the cells. We next asked whether ligand-induced GR activity altered gene expression in the groups tested (Figure 11). To that end, we treated cells with DEX, a potent and highly selective synthetic glucocorticoid. The graph only shows results for WT and transgenic MEFs, since no statistically significant effects of DEX were detected in adipocytes. In the first place, we can see that in WT MEFs *Sgk1* expression does not significantly change, while in their transgenic counterpart, after being treated with DEX, there was an increase of 4.2 times. With *Tsc22d3* happens something similar, in both WT and Tg.SGK1 MEFs, treatment with DEX resulted in a significant increase in *Tsc22d3* expression, with a higher induction in Tg.SGK1 MEFs. In contrast, *Per1* shows the opposite pattern of regulation, with a notorious increase observed in *Per1* expression in WT MEFs after DEX treatment (24.4-fold induction) and a much more modest 3.2-fold increase in Tg.SGK1 MEFs.

Taken together, it appears that acute GR effects are gene depend and likely modified by additional mechanisms that in some cases may be affected by increased SGK1 activity.

5.2. Influence of SGK1 on adipogenesis.

PPAR γ Basal Expression MEFs vs Adipocytes
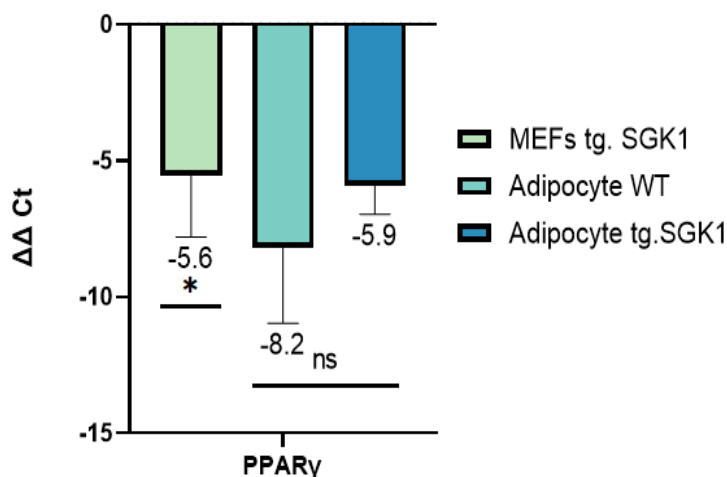
Legend: MEFs tg. SGK1; Adipocyte WT; Adipocyte tg.SGK1

Figure 13. Average difference in basal expression of Ppar*γ in the indicated cell types. * p-value < 0.05, Students T-test comparing it to MEFs WT.*

To ensure that the adipocyte differentiation protocol was successful, a lipid droplet staining protocol was performed (Figure 12). WT or Tg.SGK1 MEFs that were not supplemented with the adipogenic medium did not show lipid droplet accumulation. On the other hand, MEFs from both genotypes treated with adipogenic medium showed a clear presence of lipid droplets. Quantitative analysis of Oil-red O accumulation remains to be done in order to assess whether the transgene affects lipid accumulation during adipogenesis differentiation.

Additionally, to corroborate differentiation, we quantitated adipogenic marker gene expression. The adipogenic markers used in these samples were *Pparg* and *Cebpα.* With *Cebpα* the qPCR did not register a positive signal in any of the analysed samples. Since we did not have any positive control at our disposal to ensure that the primers were correctly designed, we cannot determine whether the absence of signal is because *Cebpα* is not expressed in the differentiated adipocytes or because primers have some kind of problem (design or production error).

On the other hand, *Pparg* primers worked as intended (Figure 13). When samples were compared to WT MEFs, basal expression of *Pparg*, all samples showed at least 32 ($2^{-\Delta\Delta Ct}$) times more basal expression of *Pparg*, with WT adipocytes having more than 250 times expression than the control. Even though the data shows a tendency towards increased levels of *Pparg* basal expression in all samples compared to WT MEFs, it must be noted that the only statistically significant data is the Tg.SGK1 MEF increase. The problem with adipocyte samples analysis is probably due to the high standard deviation of the sample's mean; because both p-values for these comparisons are 0.10. Nonetheless, the fact that *Pparγ* expression is so much higher than basal WT MEFs, alongside the lipid staining protocol, allows us to say that the adipocyte differentiation protocol was done successfully, although we cannot reach any conclusion regarding the influence of increased SGK1 activity in the process.

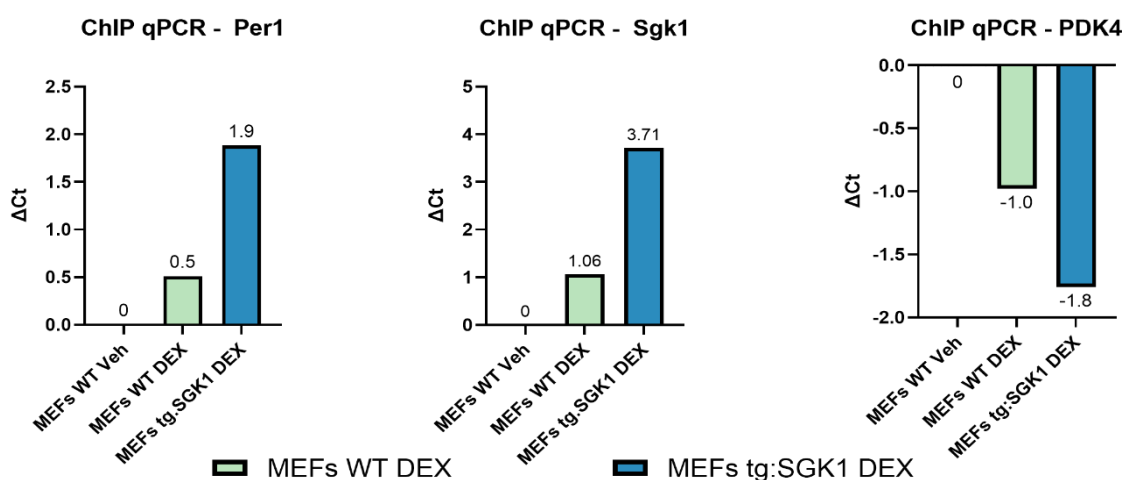## 5.3. Influence of SGK1 on GR binding to genomic GRE loci

Figure. 14. ΔCt of ChIP samples obtained from qPCR runs

We next asked whether increased SGK1 activity alters ligand-induced GR binding to chromatin. To that end, we performed ChIP reactions using a specific anti-GR antibody

using samples from WT or Tg.SGK1 MEFs treated or not with DEX. Reaction products were tested by qPCR using primer pairs flanking known GR genomic binding sites in the enhancers of GR target genes (Table 2). Figure 14 shows the results of the analysis. From the selected sites, 3 pairs of primers produced useful results. *Fkbp5* and *Amp3d* primer pairs only gave signals on the input samples, but not on the immunoprecipitated chromatin; therefore, analysis of these reactions was not possible. Another problem arose while analysing the qPCR data from the three primer pairs that worked. The immunoprecipitated sample from Tg.SGK1 MEFs treated with vehicle gave the same values as the input from that same sample, a much higher value than all other conditions, rendering that pair of data set useless for the analysis. This is the reason why Figure 14 shows only three ΔCt for each primer pair.

The analysis of the *Per1-GRE* indicates that upon DEX treatment, Tg.SGK1 MEFs WT showed higher enrichment of GR at this site compared to WT MEFs (Figure 14). The same pattern can be seen in the *Sgk1-GRE* primers, where WT MEFS showed an enrichment of 1.06 Ct while Tg.SGK1 MEFs showed an enrichment of 3.71 Ct. This indicates that upon DEX treatment GR binds with more frequency to at least certain functional GREs in the genome. This also only partially consistent with the expression data. In the case of *Sgk1*, increased binding to the GRE correlates well with increased expression in Tg.SGK1 MEFs. However, the pattern observed with *Per1* is the opposite, with higher induction of expression but lower GRE binding in Tg.SGK1 MEFs after DEX treatment. On the other hand, the *Pdk4* ChIP - qPCR analysis suggests that upon DEX stimulation, GR binds less frequently to that specific GRE.

6. CONCLUSIONS

1. Constitutively active SGK1 alters the basal expression of all GR-regulated genes tested in MEFs, but not when these cells are differentiated to adipocytes, suggesting a cell-type specific effect.
2. Acute induction of GR activity in MEFs shows gene-specific differences, suggesting that SGK1 may alter other regulatory mechanisms that differentially affect those genes.
3. We successfully stablished an adipocyte differentiation protocol using WT and transgenic MEFs. However, the effects of increased SGK1 activity on adipocyte differentiation and the role of GR in the process could not be assessed due to high variability in our results.

4. Increased SGK1 activity appears to enhance GR binding to genomic GREs, although this does not necessarily correlate to transcriptional output.
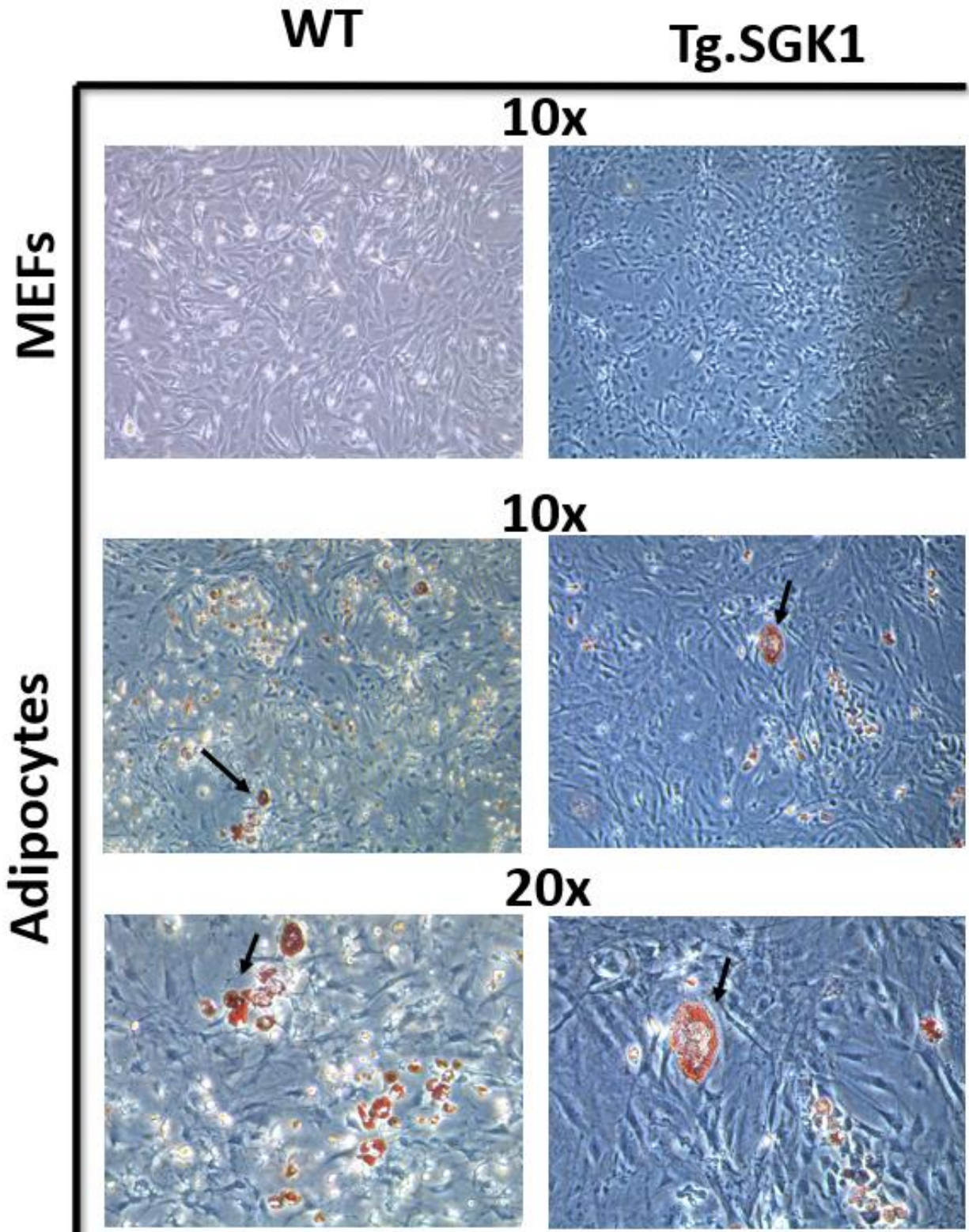

Figure 12. Images taken from differentiated adipocytes from MEFs WT and Tg.SGK1 that were treated with Oil Red-O. Arrows indicate lipid droplets produced by the cells that were stained with Oil Red-O

21

Abumrad, N. A., M. R. el-Maghrabi, E. Z. Amri, E. Lopez, y P. A. Grimaldi. 1993. «Cloning of a Rat Adipocyte Membrane Protein Implicated in Binding or Transport of Long-Chain Fatty Acids That Is Induced during Preadipocyte Differentiation. Homology with Human CD36». *The Journal of Biological Chemistry* 268 (24): 17665-68.

Alessi, Dario R., Laura R. Pearce, y Juan M. García-Martínez. 2009. «New Insights into MTOR Signaling: MTORC2 and Beyond». *Science Signaling* 2 (67): pe27. https://doi.org/10.1126/scisignal.267pe27.

Ali, Aus Tariq, Warren E. Hochfeld, Renier Myburgh, y Michael S. Pepper. 2013. «Adipocyte and Adipogenesis». *European Journal of Cell Biology* 92 (6-7): 229-36. https://doi.org/10.1016/j.ejcb.2013.06.001.

Al-Sayegh, M. A., S. R. Mahmood, S. B. Abul Khair, X. Xie, M. El Gindi, T. Kim, A. Almansoori, y P. Percipalle. 2020. «β-Actin Contributes to Open Chromatin for Activation of the Adipogenic Pioneer Factor CEBPA during Transcriptional Reprograming». Editado por Matthew Welch. *Molecular Biology of the Cell* 31 (23): 2511-21. https://doi.org/10.1091/mbc.E19-11-0628.

Bauerle, Kevin T., Irina Hutson, Erica L. Scheller, y Charles A. Harris. 2018. «Glucocorticoid Receptor Signaling Is Not Required for In Vivo Adipogenesis». *Endocrinology* 159 (5): 2050-61. https://doi.org/10.1210/en.2018-00118.

Bereshchenko, Oxana, Graziella Migliorati, Stefano Bruscoli, y Carlo Riccardi. 2019. «Glucocorticoid-Induced Leucine Zipper: A Novel Anti-inflammatory Molecule». *Frontiers in Pharmacology* 10. https://www.frontiersin.org/articles/10.3389/fphar.2019.00308.

Castel, Pau, Haley Ellis, Ruzica Bago, Eneda Toska, Pedram Razavi, F. Javier Carmona, Srinivasaraghavan Kannan, et al. 2016. «PDK1-SGK1 Signaling Sustains AKT-Independent MTORC1 Activation and Confers Resistance to PI3Kα Inhibition». *Cancer Cell* 30 (2): 229-42. https://doi.org/10.1016/j.ccell.2016.06.004.

Cerma, Krisida, Federico Piacentini, Luca Moscetti, Monica Barbolini, Fabio Canino, Antonio Tornincasa, Federica Caggia, et al. 2023. «Targeting PI3K/AKT/MTOR Pathway in Breast Cancer: From Biology to Clinical Challenges». *Biomedicines* 11 (1): 109. https://doi.org/10.3390/biomedicines11010109.

García-Martínez, Juan M., y Dario R. Alessi. 2008. «MTOR Complex 2 (MTORC2) Controls Hydrophobic Motif Phosphorylation and Activation of Serum- and Glucocorticoid-Induced Protein Kinase 1 (SGK1)». *Biochemical Journal* 416 (3): 375-85. https://doi.org/10.1042/BJ20081668.

Ghani, Madiha Javeed. 2022. «SGK1, Autophagy and Cancer: An Overview». *Molecular Biology Reports* 49 (1): 675-85. https://doi.org/10.1007/s11033-021-06836-6.

Glatz, Jan F. C., y Joost J. F. P. Luiken. 2018. «Dynamic role of the transmembrane glycoprotein CD36 (SR-B2) in cellular fatty acid uptake and utilization». *Journal of Lipid Research* 59 (7): 1084-93. https://doi.org/10.1194/jlr.R082933.

Hellal-Levy, C., B. Couette, J. Fagart, A. Souque, C. Gomez-Sanchez, y M. Rafestin-Oblin. 1999. «Specific Hydroxylations Determine Selective Corticosteroid Recognition by Human Glucocorticoid and Mineralocorticoid Receptors». *FEBS Letters* 464 (1-2): 9-13. https://doi.org/10.1016/s0014-5793(99)01667-1.

Hinds, Terry D., Sadeesh Ramakrishnan, Harrison A. Cash, Lance A. Stechschulte, Garrett Heinrich, Sonia M. Najjar, y Edwin R. Sanchez. 2010. «Discovery of Glucocorticoid Receptor-Beta in Mice with a Role in Metabolism». *Molecular*

Endocrinology (Baltimore, Md.) 24 (9): 1715-27. https://doi.org/10.1210/me.2009-0411.

Hoffman, Elizabeth A., Brian L. Frey, Lloyd M. Smith, y David T. Auble. 2015. «Formaldehyde Crosslinking: A Tool for the Study of Chromatin Complexes». *Journal of Biological Chemistry* 290 (44): 26404-11. https://doi.org/10.1074/jbc.R115.651679.

Kadmiel, Mahita, y John A. Cidlowski. 2013. «Glucocorticoid Receptor Signaling in Health and Disease». *Trends in Pharmacological Sciences* 34 (9): 518-30. https://doi.org/10.1016/j.tips.2013.07.003.

Knoedler, Joseph R., Cristina Sáenz de Miera, Arasakumar Subramani, y Robert J. Denver. 2021. «An Intact Krüppel-like Factor 9 Gene Is Required for Acute Liver Period 1 MRNA Response to Restraint Stress». *Endocrinology* 162 (9): bqab083. https://doi.org/10.1210/endocr/bqab083.

Kobayashi, T., M. Deak, N. Morrice, y P. Cohen. 1999. «Characterization of the Structure and Regulation of Two Novel Isoforms of Serum- and Glucocorticoid-Induced Protein Kinase». *The Biochemical Journal* 344 Pt 1 (Pt 1): 189-97.

LaLone, Carlie A., Daniel L. Villeneuve, Allen W. Olmstead, Elizabeth K. Medlock, Michael D. Kahl, Kathleen M. Jensen, Elizabeth J. Durhan, et al. 2012. «Effects of a Glucocorticoid Receptor Agonist, Dexamethasone, on Fathead Minnow Reproduction, Growth, and Development». *Environmental Toxicology and Chemistry* 31 (3): 611-22. https://doi.org/10.1002/etc.1729.

Lefterova, Martina I., y Mitchell A. Lazar. 2009. «New Developments in Adipogenesis». *Trends in Endocrinology & Metabolism* 20 (3): 107-14. https://doi.org/10.1016/j.tem.2008.11.005.

Orlacchio, Arturo, Michela Ranieri, Martina Brave, Valeria Antico Arciuch, Toni Forde, Daniela De Martino, Karen E. Anderson, Phillip Hawkins, y Antonio Di Cristofano. 2017. «SGK1 Is a Critical Component of an AKT-Independent Pathway Essential for PI3K-Mediated Tumor Development and Maintenance». *Cancer Research* 77 (24): 6914-26. https://doi.org/10.1158/0008-5472.CAN-17-2105.

Pavlatou, Maria G., Kasey C. Vickers, Sudhir Varma, Rana Malek, Maureen Sampson, Alan T. Remaley, Philip W. Gold, Monica C. Skarulis, y Tomoshige Kino. 2013. «Circulating Cortisol-Associated Signature of Glucocorticoid-related Gene Expression in Subcutaneous Fat of Obese Subjects». *Obesity (Silver Spring, Md.)* 21 (5): 960-67. https://doi.org/10.1002/oby.20073.

Presman, Diego M., Sourav Ganguly, R. Louis Schiltz, Thomas A. Johnson, Tatiana S. Karpova, y Gordon L. Hager. 2016. «DNA binding triggers tetramerization of the glucocorticoid receptor in live cells». *Proceedings of the National Academy of Sciences* 113 (29): 8236-41. https://doi.org/10.1073/pnas.1606774113.

Qiu, Lian, Wi Lai, Deborah Stumpo, y Perry Blackshear. 2016. «Mouse Embryonic Fibroblast Cell Culture and Stimulation». *BIO-PROTOCOL* 6 (13). https://doi.org/10.21769/BioProtoc.1859.

Sierra-Ramos, Catalina, Silvia Velazquez-Garcia, Arianna Vastola-Mascolo, Guadalberto Hernández, Nourdine Faresse, y Diego Alvarez De La Rosa. 2020. «SGK1 Activation Exacerbates Diet-Induced Obesity, Metabolic Syndrome and Hypertension». *Journal of Endocrinology* 244 (1): 149-62. https://doi.org/10.1530/JOE-19-0275.

So, Alex Yick-Lun, Christina Chaivorapol, Eric C. Bolton, Hao Li, y Keith R. Yamamoto. 2007. «Determinants of Cell- and Gene-Specific Transcriptional Regulation by

the Glucocorticoid Receptor». *PLOS Genetics* 3 (6): e94. https://doi.org/10.1371/journal.pgen.0030094.

Toska, Eneda, Pau Castel, Sagar Chhangawala, Amaia Arruabarrena-Aristorena, Carmen Chan, Vasilis C. Hristidis, Emiliano Cocco, et al. 2019. «PI3K Inhibition Activates SGK1 via a Feedback Loop to Promote Chromatin-Based Regulation of ER-Dependent Gene Expression». *Cell Reports* 27 (1): 294-306.e5. https://doi.org/10.1016/j.celrep.2019.02.111.

Toska, Eneda, Hatice U. Osmanbeyoglu, Pau Castel, Carmen Chan, Ronald C. Hendrickson, Moshe Elkabets, Maura N. Dickler, et al. 2017. «PI3K pathway regulates ER-dependent transcription in breast cancer through the epigenetic regulator KMT2D». *Science* 355 (6331): 1324-30. https://doi.org/10.1126/science.aah6893.

Webster, M. K., L. Goya, Y. Ge, A. C. Maiyar, y G. L. Firestone. 1993. «Characterization of Sgk, a Novel Member of the Serine/Threonine Protein Kinase Gene Family Which Is Transcriptionally Induced by Glucocorticoids and Serum». *Molecular and Cellular Biology* 13 (4): 2031-40. https://doi.org/10.1128/mcb.13.4.2031-2040.1993.

Weikum, Emily R., Matthew T. Knuesel, Eric A. Ortlund, y Keith R. Yamamoto. 2017. «Glucocorticoid Receptor Control of Transcription: Precision and Plasticity via Allostery». *Nature Reviews Molecular Cell Biology* 18 (3): 159-74. https://doi.org/10.1038/nrm.2016.152.

Zhu, Ruizhe, Gang Yang, Zhe Cao, Kexin Shen, Lianfang Zheng, Jianchun Xiao, Lei You, y Taiping Zhang. 2020. «The Prospect of Serum and Glucocorticoid-Inducible Kinase 1 (SGK1) in Cancer Therapy: A Rising Star». *Therapeutic Advances in Medical Oncology* 12 (enero): 175883592094094. https://doi.org/10.1177/1758835920940946.